Elucidating structural patterns in hydrogen bond dense materials: a study of ammonium salts of (4-aminium-1-hydroxybutylidine)-1,1-bisphosphonic acid.

Craig. M. Forsyth,*[a] Neil B. Greenhill,[a] Peter C. Junk[b] and Glen B. Deacon[a]

Abstract: The syntheses and structures of ammonium salts of the active pharmaceutical agent (4-aminium-1-hydroxybutylidine)-1,1-bisphosphonic acid (alendronic acid, LH_5) have been examined. Three deprotonation states of the parent acid were achieved i.e. LH_4^-, LH_3^{2-} and LH_2^{3-}, and crystallisation gave a total of six different structural phases including $[NH_4][LH_4]\cdot 2(H_2O)$ as two polymorphs **1a** and **1b**, two hydrates of $[NH_4]_2[LH_3]\cdot x(H_2O)$, x = 3 (**2**), x = 6 (**3**), $[NH_4]_4[OH_3][LH_3][LH_2]\cdot 8(H_2O)$ (**4**) and $[NH_4]_3[LH_2]\cdot 3(H_2O)$ (**5**). The crystal structures obtained, along with that of the parent acid, enable a direct comparison of competing supramolecular synthons, involving phosphonate-phosphonate O-H···O and ammonium-phosphonate N-H···O hydrogen bonds, in a series displaying progressively decreasing P-OH with concomitantly increasing RNH_3^+ moieties. Indeed, the structures show some consistent connectivity patterns of the alendronate units, which thus assemble into substructures such as 2-D sheets ($LH_5\cdot H_2O$, **1a**), zig-zag chains (**2**, **5**) or ladder-like arrays (**3**, **4**). The occurrence of these motifs appears to correlate with the ionisation level of the parent acid.

Introduction

The ability to fine tune the chemistry of active pharmaceutical agents can have significant benefits in terms of both their therapeutic properties such as bioavailability, as well as physiochemical properties, such as stability and solubility. For acidic pharmaceuticals, modification of the original molecules has been readily achieved by the formation of salts, both with simple counterions, e.g. Na^+, K^+, NH_4^+,[1] as well as incorporating more elaborate multi-drug salt systems[2] and ionic liquid pharmaceuticals.[3,4] Bisphosphonates, i.e. molecules possessing a geminal $R_2C(PO_3)_2$ fragment, are an important class of therapeutic agents in current clinical use for the treatment of bone disorders.[5] Furthermore, studies have also shown that bisphosphonates may interact with key enzymes enabling a wider variety of disease therapies.[6-12] Alendronic acid, (4-aminium-1-hydroxybutylidine)-1,1-bisphosphonic acid (LH_5) and pamindronic acid (3-aminium-1-hydroxypropylidine)-1,1-bisphosphinic acid (L^1H_5) are commercially available and efficacious treatments for osteoporosis.[6] These molecules have a hydroxy and an alkylamine group substituted on the geminal carbon and have five acidic protons, with pK_a values in the range 0.8 to 12.2.[13,14] Both exist as a zwitterions in the solid state through transfer of a phosphonate hydrogen atom to the amine group.[15,16,17] Due to their biological relevance, the structures of alkali and alkaline earth metal and copper and zinc salts, in either the monoanionic LH_4^-or $L^1H_4^-$ or the dianionic forms LH_3^{2-}or $L^1H_3^{2-}$ have been studied.[18-26] Apart from monomeric $[Li(LH_4)(H_2O)_2]$[20] these compounds generally form very complex coordination polymers in the solid state with limited solubility in water, apart from the alkali metal salts. Even so, coordination polymers of metal alendronate and pamindronate complexes have been studied as pH-induced slow release delivery systems for bisphosphonates, as well as for their inherent bioactivity.[27-29] Diverging from the use of metal salts, there has been interest in the organic salts of bisphosphonates. These can take the form of acid-base systems, usually with amines as the hydrogen acceptors,[30-34] including nucleobases[30,31] and other biocompatible cations.[33,34] Significantly, examples of organic salts of alendronate materials were shown to be highly soluble, and cytotoxic against various cancer cell lines.[34]

An intrinsic feature of bisphosphonates is the notable structural influence of the supramolecular interactions derived from strong P-OH···O hydrogen bonds, typically between phosphonate groups.[35,36] These are often observed in cyclic $\boldsymbol{R_2^2}(8)$ or $\boldsymbol{R_2^2}(12)$ motifs (by graph set notation[37]).[38,39] However, for alendronate compounds, there are additional charge assisted N-H···O interactions resulting from the butylaminium group. Notwithstanding the complexity in these systems, there is emerging evidence that both these types of interactions can significantly impact upon the observed structures of alendronate salts. For example, we have previously shown that the complexes, $[Na(LH_4)(H_2O)]\cdot 2(H_2O)$ and $[Cs(LH_4)(H_2O)]\cdot H_2O$ have the same hydrogen bonded alendronate-alendronate connectivity and similar overall structures, despite differing metal-coordination requirements (Na = CN 6, Cs = CN 9).[22] We have also demonstrated the occurrence of head to tail N-H···O-P bonded alendronate aggregates in a series of organoaminium salts of the form $[RNH_3]_2[LH_3]$ or $[H_3NR'NH_3][LH_3]$.[32] Furthermore, recurring substructures were observed with differing cations, suggesting that there may be some persistent structural motifs.[32] In order to look more closely at the supramolecular chemistry of alendronate systems we have now investigated the syntheses and structures of a series of ammonium salts of alendronic acid. Previous studies of liposome encapsulated pharmaceuticals have utilised

[a] Dr. C. M. Forsyth, Dr. N. B. Greenhill, Prof. G. B. Deacon
School of Chemistry
Monash University
Clayton, Victoria 3800, Australia
E-mail: craig.forsyth@monash.edu
[b] Prof. P. C. Junk
College of Science and Engineering
James Cook University
Townsville, Queensland 4811, Australia

Supporting information for this article is given via a link at the end of the document.

$[NH_4]_2[LH_3]$ as an alendronate source.[40,41] This salt was prepared by neutralisation of the acid with ammonium hydroxide to pH 6.0 but was used *in situ* and was not isolated. Ammonium salts of the related bisphosphonates risendronic acid (L^2H_5), and zolendronic acid (L^3H_5), e.g. $[NH_4][L^2H_4]\cdot 2(H_2O)$ and $[NH_4]_2[L^3H_3]\cdot 2(H_2O)$, have been prepared similarly, and structurally characterised.[42,43] In the current study we now report three deprotonation states of alendronic acid LH_4^-, LH_3^{2-} and LH_2^{3-}, yielding six different structural phases: $[NH_4][LH_4]\cdot 2(H_2O)$ as two polymorphs **1a** and **1b**, two hydrates of $[NH_4]_2[LH_3]\cdot x(H_2O)$, x = 3 (**2**), or x = 6 (**3**), $[NH_4]_4[OH_3][LH_3][LH_2]\cdot 8(H_2O)$ (**4**) and $[NH_4]_3[LH_2]\cdot 3(H_2O)$ (**5**). Each of these structures displays a complex 3-D network with an abundance of hydrogen bond interactions. These structures, along with that of $LH_5\cdot H_2O$, provide an opportunity to compare the influence of various supramolecular interactions in a series of related compounds that have either three, two, one or zero P-OH moieties.

Results and Discussion

Syntheses The syntheses of the ammonium salts of of 4-aminium-1-hydroxybutylidine)-1,1-bisphosphonic acid (LH_5) were readily achieved by neutalisation of the acid with aqueous ammonium hydroxide. The relevant acidity constants for LH_5 are pK_2 2.2, pK_3 6.3 and pK_4 10.9,[13] which allow for pH control of the ionisation level of the acid. The 1:1 salt, $[NH_4][LH_4]$ was thus obtained from reactions of $LH_5\cdot H_2O$ and aq. NH_3 in water to a final pH of *ca* 5, and the product was crystallised from water/EtOH with the composition $[NH_4][LH_4]\cdot 2(H_2O)$ **1a** (Scheme 1). Alternatively, solid NH_4HCO_3 could also be used as a stoichiometric deprotonation reagent, similarly giving **1a** in good yield (Scheme 1). However, an analogous preparation using $(NH_4)_2CO_3$ was less satisfactory and yielded impure **1a**, as an initial product. The impurity was shown to be unreacted $LH_5\cdot H_2O$ by PXRD. Subsequently, a smaller amount of a second crystalline product was obtained after isolation of the initial material, and which was shown to be a mixture of **1a** and the structural polymorph **1b**. However, **1b** was not obtained as a single phase. The 2:1 salt, $[NH_4]_2[LH_3]$ was prepared by addition of an excess of NH_3 to $LH_5.H_2O$ in water giving a final pH value of *ca* 9-10. The initial product was crystallised as very fine needles by addition of EtOH to the cooled reaction solution. Re-crystallisation of this material by cooling a hot water/DMSO solution to room temperature, yielded well-formed prismatic crystals of the trihydrate $[NH_4]_2[LH_3]\cdot 3(H_2O)$ (**2**). The composition of this product was confirmed by elemental analysis, whereas comparative data for the initially obtained needles suggested that these were a higher hydrate e.g. $[NH_4]_2[LH_3]\cdot x(H_2O)$, x ≈ 5. Subsequently, PXRD showed this product to be a mixture of $[NH_4]_2[LH_3]\cdot 6(H_2O)$ (**3**) and $[NH_4]_4[OH_3][LH_3][LH_2]\cdot 8(H_2O)$ (**4**) by comparison with the calculated patterns obtained from the crystal structures (see below). A reaction of $LH_5.H_2O$ with a larger (×5) excess of NH_3 in water (final pH *ca* 12) also yielded **2**, in this case directly from the reaction mixture upon addition of DMSO. In contrast, the reaction of $LH_5\cdot H_2O$ with undiluted 28% aq. NH_3 gave instead the 3:1 compound $[NH_4]_3[LH_2].3(H_2O)$ (**5**) as a voluminous solid which was isolated in good yield by rapid filtration and drying. As a solid, **5** appeared to be stable in a sealed vial for several days, but subsequently PXRD indicated that significant decomposition into **4** had occurred after 1 month and this was reflected in a low %N content in the elemental analysis for **5**. Furthermore, the initial reaction mixture, when left as a suspension for 2-5 days, also partially converted into a mixture containing well-formed crystals of compounds **5**, **4** and **3**. These mixtures were insoluble in aq. NH_3 and could be isolated by filtration. However, the suspension, after a period of five days, mostly dissolved and subsequently the 2:1 salt **2** was isolated from the filtrate in good yield as the major product. IR spectra of **1a**, **2** and **5** showed absorptions between 1200-900 cm^{-1}, indicative of the phosphonate groups. In the 3500-2500 cm^{-1} region, and a complex series of bands overlay a very broad absorption, consistent with strong hydrogen bonding.

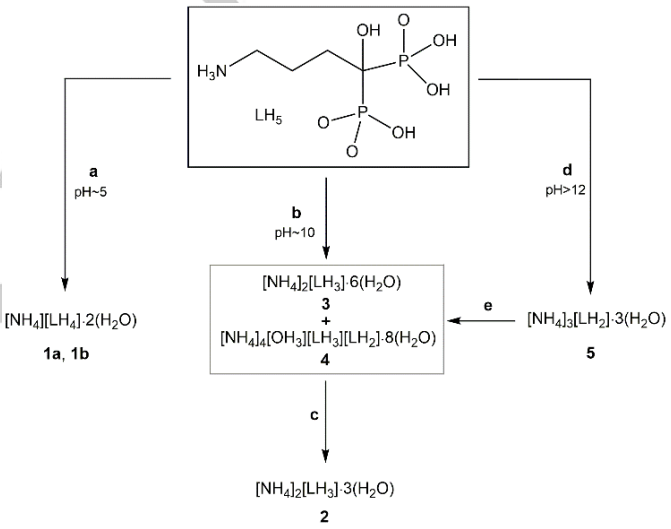

Scheme 1. Syntheses of ammonium salts of alendronic acid. a) 1:1 $LH_5.H_2O$:28% NH_3, or 1:1 $LH_5\cdot H_2O$:NH_4HCO_3 or 2:1 $LH_5\cdot H_2O$:$(NH_4)_2CO_3$, H_2O. b) 1:2 $LH_5\cdot H_2O$:28% NH_3, H_2O. c) recrystallisation from H_2O/DMSO. d) 28% NH_3, 20 min. e) standing 2-5 days.

Crystal Structure Analysis Each of the structures described below comprises a zwitterionic alendronate moiety, having a protonated butylaminium group, RNH_3^+ with either one RPO_3H_2 and one RPO_3H^- (LH_5), two RPO_3H^- ($[NH_4][LH_4]$ **1a, 1b**), one RPO_3H^- and one RPO_3^{2-} ($[NH_4]_2[LH_3]$ **2**, **3**) or two RPO_3^{2-} groups ($[NH_4]_3[LH_2]$ **5**) (note: compound **4** was modelled as having one LH_3^{2-} and one LH_2^{3-} anion). The crystal structure of $LH_5\cdot H_2O$ has been reported previously by Leroux in 1991 (CSD KOJGUL) and showed two independent, but pseudo-symmetric, LH_5 molecules.[15] However, the room temperature data revealed only three of the six acidic P-OH hydrogen atom positions and consequently we have redetermined the crystal structure at 123 K (see Supplementary Information) for direct comparison with the current data. The structure of $LH_5\cdot H_2O$ comprises a 3-D network of zwitterionic molecules connected by 19 unique hydrogen bonds. Using the definition of Steiner for a strong hydrogen bond (D···A ≤ *ca* 2.5 Å),[44] all six P-OH moieties are involved in strong

interactions. Five of these are between phosphonate groups, forming a 3-D network of interconnected $\boldsymbol{R_4^4}(20)$ ring systems (Figure 1). It should be noted that for each ring system there are two variants corresponding to differing hydrogen atom positions within the rings. The remaining P-OH moiety forms a very strong hydrogen bond to a water molecule, O(16) (Table S1). There are analogous $\boldsymbol{R_4^4}(20)$ ring systems present in the structures of anhydrous LH_5,[15] the related pamidronic acid L^1H_5,[17] as well as in the structures of $[Na(LH_4)(H_2O)]\cdot 2(H_2O)$, and phase II $[M(LH_4)(H_2O)]\cdot(H_2O)$, M = Rb and Cs), despite the coordination of the alendronate by the metal cations in these instances.[22] Additionally, $LH_5\cdot H_2O$ contains 2-D monolayers of aligned LH_5 molecules lying parallel to the *ac* plane (Figure 2). In these layers, each LH_5 is linked through one O-H···O (phosphonate-phosphonate) and two N-H···O (butylaminium-phosphonate and butylaminium-alcohol) hydrogen bonds.

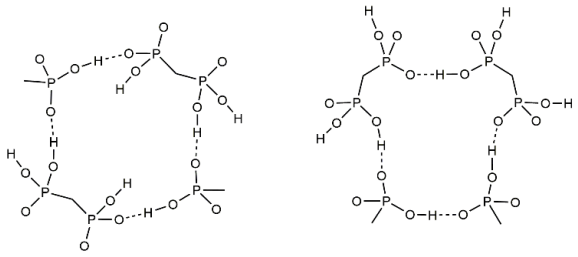

Figure 1. Schematic representation of P-OH···O ring motifs in $LH_5\cdot H_2O$ showing the two unique $\boldsymbol{R_4^4}(20)$ ring systems.

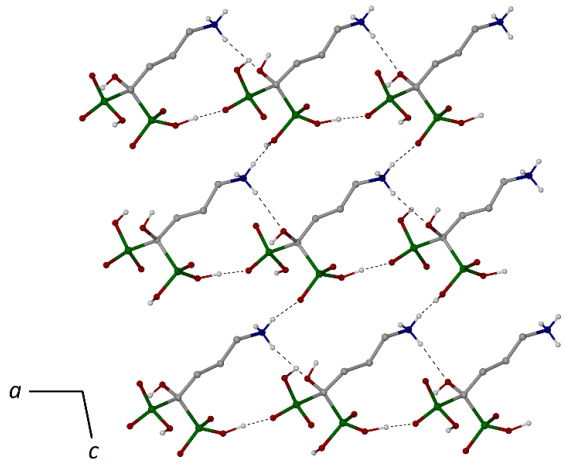

Figure 2 A view of part of the structure of $LH_5\cdot H_2O$ showing the 2-D sheet substructure, as viewed perpendicular to the *ac* plane. Water molecules have been omitted for clarity.

The structure of the first polymorph of $[NH_4][LH_4]\cdot 2(H_2O)$ **1a** comprises a single unique LH_4^- anion with a NH_4^+ counter ion and two water molecules, connected into a 3-D network by 15 unique hydrogen bonds. The connectivity between LH_4^- anions is interesting and remarkably similar to that of $LH_5\cdot H_2O$, where 1a contains 2-D monolayers of aligned LH_4^- anions parallel to the *ac* plane with the same supramolecular connectivity (Figure 3). Significantly, the P-OH···O-P interactions are stronger in the acid D···A: $LH_5.H_2O$, O(5)···O(9) 2.4790(11), O(11)···O(1^{iii}) 2.4218(11) Å, ^{iii}x-1,y,z; *cf* **1a**, O(1)···O(6^{i}) 2.5701(15) Å, ^{i}x+1,y,z) whereas the N-H···O (butylaminium-phosphonate) interaction is stronger in the ammonium salt (D···A: $LH_5\cdot H_2O$, N(1)···O(4^{ii}) 2.7962(13), N(2)···O(12^{ii}) 2.8518(13) Å, ^{ii}x-1/2,3/2-y,z-1/2; *cf* **1a** N(1)···O(3^{iv}) 2.6582(17) Å, ^{iv}x+1,3/2-y,1/2+z). Underlying the structure of **1a**, there is a $\boldsymbol{R_4^4}(20)$ ring connectivity of the bisphosphonate groups, also similar to that of acid $LH_5\cdot H_2O$, but with additional $\boldsymbol{R_2^2}(8)$ ring motifs of P-OH···O hydrogen bonds (D···A: 2.6339(16) Å) between two symmetry related phosphonate groups (Figure 4). When the structure of **1a** is viewed down the *a* axis (Figure 5), the 2-D sheet substructures stack along the *b* axis, interposed by the NH_4^+ cations and water molecules. The connectivity between the layers of LH_4^- anions comprises the aforementioned $\boldsymbol{R_2^2}(8)$ ring motif between phosphonate groups (**A** in Figure 5), as well as a $\boldsymbol{R_4^2}(8)$ ring system comprising two symmetry related water molecules, O(8), and two P-O moieties (**B** in Figure 5). The NH_4^+ cation and the remaining water molecule, O(9) form a N-H···O hydrogen bonded pair lying in channels parallel to the *a* axis (Figure 5) and held by six further hydrogen bonds, two N-H···O to phosphonate groups, one N-H···O to an alcohol group, two O-H···O from water to phosphonate groups and one O-H···O from the alcohol group to the water molecule (Table S2).

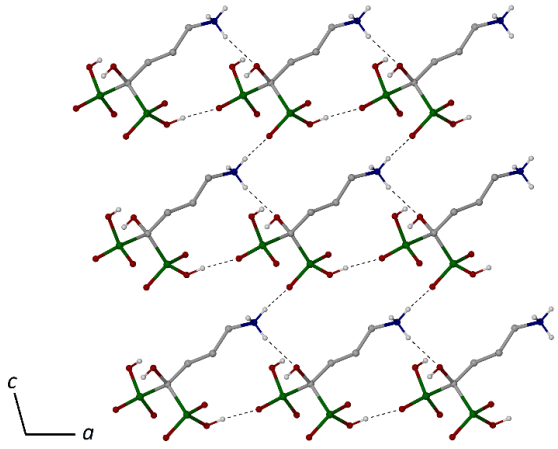

Figure 3. A view of part of the structures of $[NH_4][LH_4]\cdot 2(H_2O)$ **1a**, showing the 2-D sheet substructure, as viewed perpendicular to the *ac* plane, Water molecules and the NH_4^+ cations have been omitted for clarity.

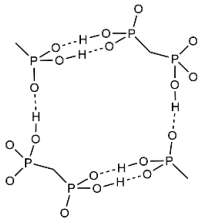

Figure 4. Schematic representation of P-OH···O ring motifs in **1a**, showing the two unique $\boldsymbol{R_4^4}(20)$ ring system, supported by two $\boldsymbol{R_2^2}(8)$ motifs.

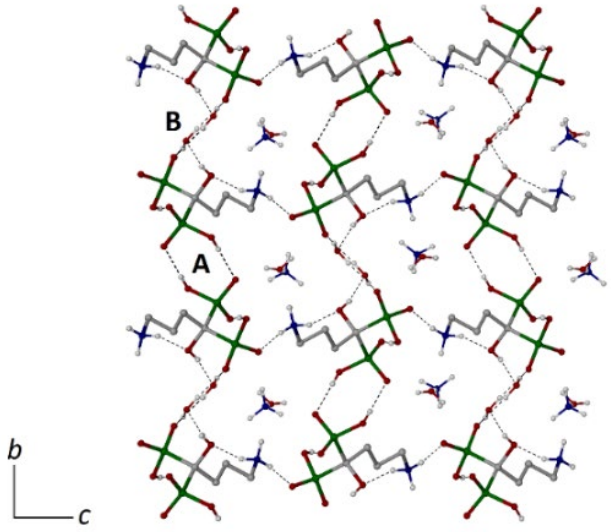

Figure 5. Packing diagram of **1a**, as viewed down the *a* axis. Some hydrogen atoms and some hydrogen bonds have been omitted for clarity. The bisphosphonate connectivity between the 2-D layers of LH_4^- molecules comprises **A**, a $\boldsymbol{R}_2^2(8)$ ring motif between two PO_3H^- groups and **B**, a $\boldsymbol{R}_4^2(8)$ ring motif involving two water molecules and two P-O moieties.

The structure of the second polymorph of $[NH_4][LH_4]\cdot 2(H_2O)$ **1b** is similarly a 3-D hydrogen bonded network, but the arrangement is much more complex. There are two structurally unique LH_4^- anions with differing $-CH_2CH_2CH_2NH_3^+$ chain conformations, one antiperiplanar (as for **1a** above) and one gauche, in addition to two NH_4^+ cations and four water molecules with a total of 28 unique hydrogen bonds (Table S3). The two different LH_4^- anions are each assembled into a ladder-like substructure with differing connectivity as a consequence of the butyl chain conformation. The first comprises a head-to-tail array of LH_4^- anions, connected on each side by two N-H···O hydrogen bonds and supported by a water molecule bridging between two phosphonate groups, and tethered by a C-OH···O interaction (Figure 6a). Notably a similar ladder motif is also observed in compounds **3** and **4** below. The second LH_4^-/H_2O ladder array retains the bridging water molecule, but the two N-H···O hydrogen bonds of the butylaminium group bind instead to one phosphonate group and to the water molecule. On each side of the ladder there is a strong O-H···O phosphonate-phosphonate interaction (D···A: O(9)···O(13^{iv}) 2.4682(15) Å, ^{iv}x,y+1,z) resulting from a change in orientation of the bisphosphonate fragment relative to the those in the first ladder (Figure 6b). When viewed down the *b* axis (Figure 7) the ladder substructures are arranged into an alternating 2-D array. The underlying phosphonate connectivity, mediated by P-OH···O hydrogen bonds, is significantly different to that observed in $LH_5\cdot H_2O$ or **1a** above, and comprises a $\boldsymbol{R}_3^3(10)$ (**A** in Figure 7) and a $\boldsymbol{R}_2^2(8)$ (**B** in Figure 7) ring system. The P-OH···O interactions are generally shorter than in **1a** above (D···A: 2.4584(14) – 2.6166(15) Å). In addition, there are three further phosphonate acceptor interactions which interconnect the ladder substructures, one with the alcohol group (O(14), D···A: 2.6817(16) Å), forming a $\boldsymbol{R}_2^2(10)$ ring system with a symmetry equivalent (**C** in Figure 7), and two N-H···O interactions with N(1) and N(2) (D···A: 2.7271(17), 2.7380(17) Å). Remarkably, the overall structure shows a close relationship with that of phase I of $[Rb(LH_4)(H_2O)]\cdot H_2O$ where the Rb^+ atoms lie in the same positions as the NH_4^+ cations in the current structure (see Supplementary Information, Figure S1).[22] In **1b**, one NH_4^+ cation binds to four separate phosphonate groups from three LH_4^- anions (D···A: 2.8089(17) – 2.9228(17) Å) whilst the second binds to two phosphonate groups and one alcohol group from three LH_4^- anions (D···A: 2.7907(19) – 3.0608(19) Å), with the final interaction to a water molecule (D···A: 2.803(2) Å). These D···A distances are within the range observed for the Rb-O distances in phase I of $[Rb(LH_4)(H_2O)]\cdot(H_2O)$ (2.808(2) – 3.252(2) Å).[22]

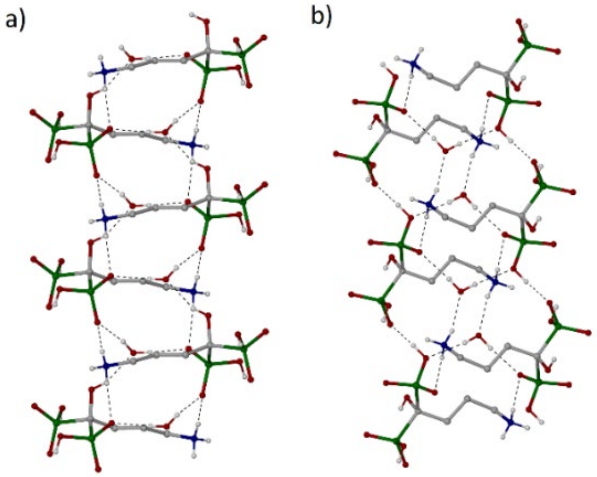

Figure 6. A view or part of the structure of **1b**, showing the two unique ladder-like structures running parallel to the *b* axis.

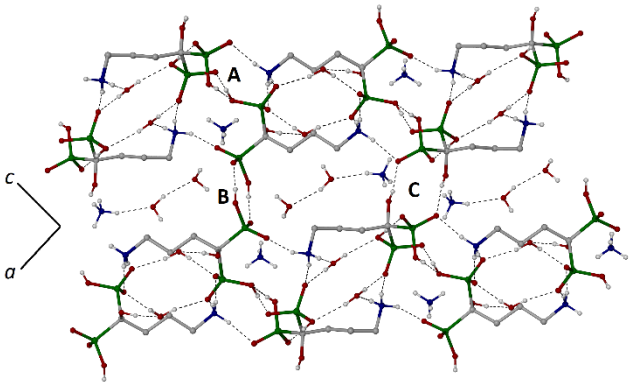

Figure 7. Packing diagram of **1b**, as viewed down the *b* axis. Some hydrogen atoms and some hydrogen bonds have been omitted for clarity. **A** denotes the a $\boldsymbol{R}_3^3(10)$ ring motif between three PO_3H^- groups; **B** denotes the $\boldsymbol{R}_2^2(8)$ ring motif involving two PO_3H^- groups; **C** comprises the $\boldsymbol{R}_3^3(10)$ ring motif between symmetry related PO_3H^-/COH pairs.

The dominant phase in the 2:1 $[NH_4]_2[LH_3]$ system is $[NH_4]_2[LH_3]\cdot 3(H_2O)$ compound **2**. In this structure, the sole P-OH moiety participates in a strong intra-molecular O-H···O hydrogen bond (D···A: O(5)···O(2) 2.5026(16) Å) linking the PO_3H^- and PO_3^{2-} groups, effectively eliminating the phosphonate P-OH donor from contributing to the 3-D connectivity. Consequently, it is therefore not surprising that the structure of **2** is remarkably similar to that of the 3:1 compound $[NH_4]_3[LH_2]\cdot 3(H_2O)$ **5** which is devoid of a P-OH moiety (see below). The structure of **2** comprises a single unique LH_3^{2-} anion with two NH_4^+ cations and three water molecules held by 19 hydrogen bonds (Table S4). For the structure of **5**, there are a LH_2^{3-} anion with three NH_4^+ cations and three water molecules resulting in 22 hydrogen bonds (Table S7). Both structures exhibit the same 2-D layers of LH_3^{2-} or LH_2^{3-} anions and some water molecules lying parallel to the *bc* plane with the phosphonate groups on the outer surfaces and the NH_4^+ and remaining water molecules sandwiched in between (Figures 8 and 9). The 2-D layers are built from identical zig-zag chains of LH_3^{2-} or LH_2^{3-} anions parallel to the *b* axis, where individual anions are linked via N-H···O-P hydrogen bonds and a water molecule, O(8), that bridges neighbouring phosphonate groups (Figure 10a). These chains are assembled along the *c* axis into a 2-D layers through (i) a C-O-H···O-P hydrogen bond, (ii) an additional water molecule, O(9), that forms a bridge between two phosphonate groups and (iii) two N-H···OH_2 hydrogen bonds to the bridging water molecules, O(8) and O(9) (Figure 10b). Each of these hydrogen bonds have D···A distances in the range 2.7128(11)-2.8524(17) Å for **2** and 2.6903(15)-2.8822(15) Å for **5**, with the phosphonate/water interactions generally the shorter.

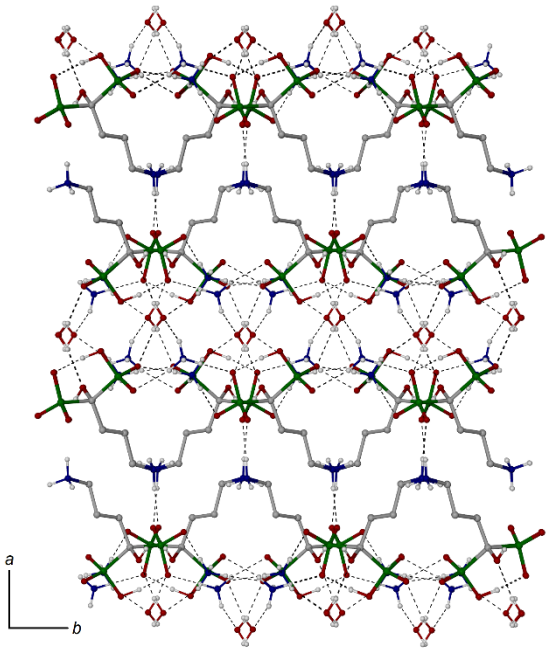

Figure 8. Packing diagrams of compound **2**, as viewed down the *c* axis (some water molecules have been omitted for clarity).

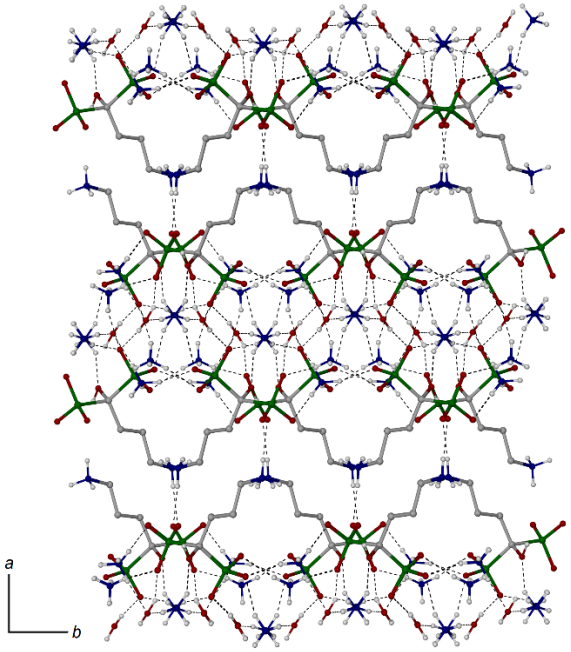

Figure 9. Packing diagrams of compound **5**, as viewed down the *c* axis (some water molecules have been omitted for clarity).

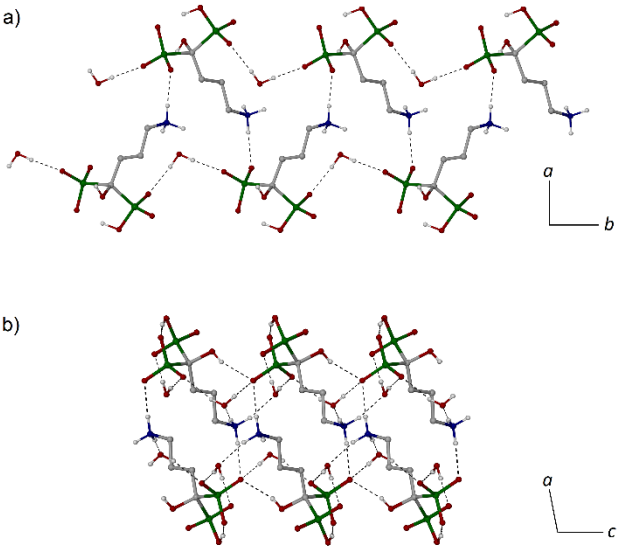

Figure 10. Part of the structure of **2** showing (a) the zig-zag chain of LH_3^{2-} anions along the *b* axis, and (b) side view of the individual chains which assemble into a 2-D sheet through interactions along the *c* axis. The structure of compound **5** is identical, apart from the phosphonate hydrogen atom which is absent in **5**.

Some of the inter-layer connectivity is the same for both compounds **2** and **5**, with two phosphonate groups from neighbouring LH_3^{2-} or LH_2^{3-} anions bridged by two NH_4^+ cations, N(2) and N(3), and a water molecule O(8) (Figure 11a,b). Both the NH_4^+ cations in **2** additionally bind to a further phosphonate

group (not shown) as well as a water molecule, O(10) (Figure 11a). This water molecule also binds to a phosphonate group from one layer and an alcohol group from the next layer. For compound **5**, the third NH_4^+ cation, N(4), lies in between the layers and binds to phosphonate group from one layer and an alcohol group from the next layer, mimicking the structural role of the water molecule O(10) in compound **2** (Figure 11b). Here the similarities with compound **2** end, with the central NH_4^+ cation also binding to a further phosphonate group (not shown) and the additional water molecule O(10) (Figure 11b). Overall, the structures of **2** and **5** parallel that of the related organoaminium alendronate salts $[enH_2][LH_3]\cdot 2(H_2O)$, $[odaH_2][LH_3]\cdot 2(H_2O)\cdot 0.5(EtOH)$ (oda = 1,8-octanediamine) and $[PheaH]_2[LH_3]\cdot 2(H_2O)$ (Phea = phenylethylamine) which have identical 2-D LH_3^{2-}/H_2O layers.[32] This is remarkable given, for example in $[PheaH]_2[LH_3]\cdot 2(H_2O)$, the interlayer region is hydrophobic, containing solely the $PhCH_2CH_2$ groups, in contrast to the hydrophilic nature of compounds **2** and **5**. In $[enH_2][LH_3]\cdot 2(H_2O)$ the $NH_3CH_2CH_2NH_3^{2+}$ dication is bound vertically between the layers, in a similar arrangement to the supramolecular $NH_4^+\cdots OH_2\cdots NH_4^+$ chain in **2** and **5** (Figure 11a,b). The analogous zolendronate salt $[NH_4]_2[L^3H_3]\cdot 2(H_2O)$, is also composed of 2-D $L^3H_3^{2-}$ layers with the NH_4^+ and water molecules sandwiched in between, although the intermolecular $L^3H_3^{2-}$ bonding is significantly different.[43]

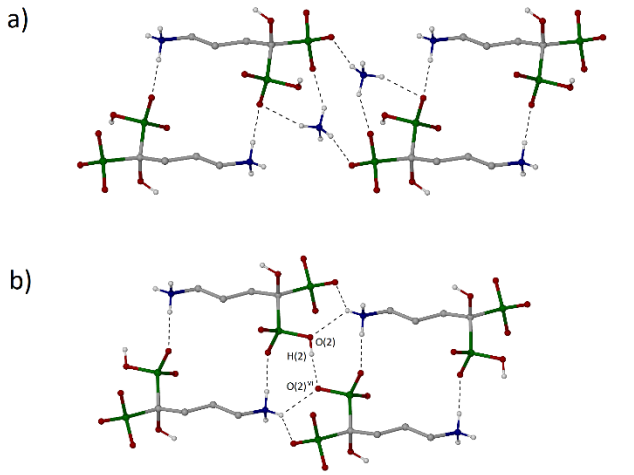

Figure 11. Part of the structures of **2** and **5** showing the NH_4^+ cation connectivity in a) **2** and b) **5**.

The two remaining structures of compounds **3** and **4**, which were observed as intermediate phases in the preparations of both **2** and **5**, have a higher number of water molecules which results in a different structural motif. Both structures possess a ladder-like substructure of alednronate anions which are assembled through two self-complementary butylaminium-phosphonate N-H···O hydrogen bonds (D···A: **3** 2.7692(17) Å; **4** 2.8125(14) Å), and supported by two bridging water molecules with two O-H···O hydrogen bonds to phosphonate groups forming a $\boldsymbol{R_4^4}(12)$ ring motif (D···A: **3** 2.7195(16), 2.8272(17) Å; **4** 2.6589(13), 2.6938(13) Å) (Figure 12). There is an additional CO-H···O interaction between the alendronate anion and the bridging water molecule (D···A: **3** 2.7413(17) Å; **4** 2.8333(13) Å). This same ladder motif was previously observed in the structure of $[m\text{-}C_6H_4(CH_2NH_3)_2][LH_3]\cdot 4(H_2O)$.[32]

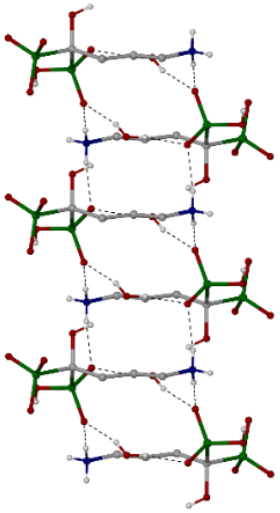

Figure 12. Ladder-like substructure of LH_3^{2-} anions and water molecules present in the structures of both compounds **3** and **4**.

For compound **3**, neighbouring ladder substructures are connected solely through the bridging NH_4^+ cations (Figure 13a) with the phosphonate hydrogen atom bonded to a water molecule within the framework cavity (see below), However, for compound **4**, the connectivity is more complex. In this case, the ladders are connected by two pairs of bifurcated N-H···O hydrogen bonds from two butylaminium groups and two phosphonate groups in a planar ring system that has additionally a strong phosphonate-phosphonate O-H···O hydrogen bond (D···A: $O(2)\cdots O(2^{vi})$ 2.4530(18) Å) (Figure 13b). In the latter interaction, the hydrogen atom attached to O(2) is modelled at half-occupancy. Thus the $O(2)\text{-}H(2)\cdots O(2^{vi})$ forms a disordered O-H···O system, with the hydrogen atom attached at either O(2) or $O(2^{vi})$. The complementary disorder component is a half-occupancy H_3O^+ cation located in the framework cavities (see below), yielding the overall structural model $[NH_4]_4[OH_3][LH_3][LH_2]\cdot 8(H_2O)$. In addition to the above ring system, the ladder substructures in **4** are also connected by two symmetry related NH_4^+ cations, N(3) located above and below the planar ring system (not shown in Figure 13b), that each bridge to three phosphonate groups by N-H···O hydrogen bonds (D···A: 2.7595(15) – 3.0045(15) Å). In both structures, the connectivity of the ladders results in 2-D layers parallel to the *ac* plane for **3** or the *ab* plane for **4**, and these are connected into a 3-D network though the second NH_4^+ cation, via three N···O hydrogen bonds to phosphonate groups (Figures 14 and 15, Tables S5 and S6). Both these 3-D LH_3^{2-}/NH_4^+ scaffolds

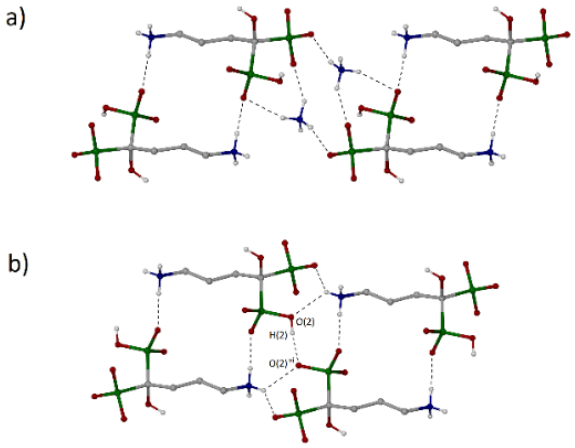

Figure 13. (a) Part of the structure of **3** showing the phosphonate–butylaminium connectivity between neighbouring ladders. (b) part of the structure of **4** showing the phosphonate–butylaminium connectivity between neighbouring ladders; (symmetry op: ^{vi}1-x,1-y,1-z).

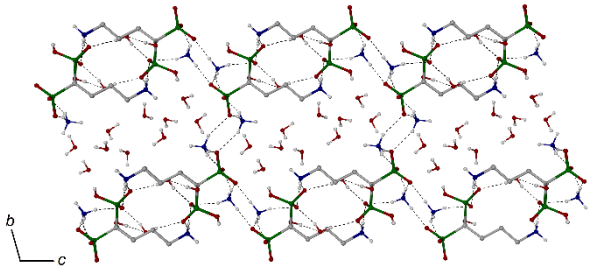

Figure 14. The extended structure of **3**, as viewed down the length of the ladder substructures and showing the linear cavities parallel to the *a* axis containing the lattice H_2O molecules. Some hydrogen bonds have been omitted for clarity

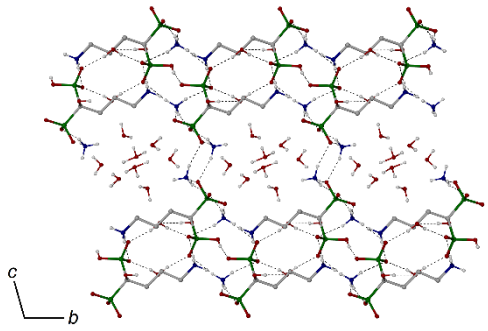

Figure 15. The extended structure of **4**, as viewed down the length of the ladder structures and showing the linear cavities parallel to the *a* axis containing the lattice H_2O molecules and H_3O^+cations. Some hydrogen bonds have been omitted for clarity.

surround channels along the *a* axis which contain the remaining water molecules. The subtle changes in the bonding between the two structures, described above, results in a larger cavity volume for compound **3** (236.5 Å^3 per unit cell) compared to compound **4** (201.8 Å^3 per unit cell), allowing for the increased degree of hydration in compound **3**.

Conclusions

The syntheses of compounds of the type $[NH_4][LH_4]$, $[NH_4]_2[LH_3]$ can be readily achieved from simple reagents and the products obtained appear to be stable and are considerably more soluble than the parent acid. Crystalline solid phases as hydrates, $[NH_4][LH_4]\cdot 2(H_2O)$ **1a** and $[NH_4]_2[LH_3]\cdot 3(H_2O)$ **2** were isolated in good yields and fully characterised. These well-defined compounds are ideal candidates for use as pharmaceutical agents.[36,37] A polymorph of $[NH_4][LH_4]\cdot 2(H_2O)$ **1b** and two further hydrates $[NH_4]_2[LH_3]\cdot 6(H_2O)$ **3** and $[NH_4]_4[OH_3][LH_3][LH_2]\cdot 8(H_2O)$ **4** and were crystallised under some conditions, but these were not isolated as pure phases. The unusual compound $[NH_4]_3[LH_2]\cdot 3(H_2O)$ **5** was also obtained but was shown to be unstable both in solution and in the solid state. Whilst structurally interesting, compound **5** is not practical as a pharmaceutical ingredient. However it may be possible to stabilize the LH_2^{3-} anion with other counter ions, similar to the analogous zolendronate species $[cy_2NH_2]_3[L^3H_2]\cdot H_2O\cdot EtOH$.[44]

The structures of the ammonium salts of alendronic acid that are described here are each highly complex, 3-D hydrogen bonded networks but they can be classified into two broad groups according to the ionization level of the alendronate moiety. Firstly, those corresponding to the parent acid $LH_5\cdot H_2O$ and the more commonly obtained phase of $[NH_4][LH_4]\cdot 2(H_2O)$ **1a**. These structures contain similar 2-D layers of hydrogen bonded LH_5 molecules or LH_4^- anions and both have structurally significant, P-OH···O-P interactions and both have the $\boldsymbol{R_4^4}(20)$ ring connectivity between four alendronate moieties. The second broad structural classification comprises those containing the more ionized alendronate LH_3^{2-} and LH_2^{3-} anions, compounds **2**, **3**, **4** and **5**. Within this group of structures there are two variants, both of which have the same head-to-tail alendronate binding mediated by N-H···O-P hydrogen bonds and water molecules bridging between phosphonate groups but in two distinct arrangements. The first comprises a zig-zag chain substructure element (**2**, **5**) whilst the second comprises an infinite ladder-like substructure (**3**, **4**). The only exception to the above classifications is the second polymorph of $[NH_4][LH_4]\cdot 2(H_2O)$ **1b** which has several unique features including two butylaminium chain conformations and differing P-OH···O-P connectivity. However, overall the structures presented here provide further evidence for the existence of stable alendronate structural motifs that persist in the LH_5/[cation][LH_4] or [cation]$_2$[LH_3]/[cation]$_3$[LH_2] systems with differing cations, despite the complexity of the supramolecular interactions.

Experimental Section

Alendronic acid monohydrate was generously provided by a commercial pharmaceutical company and was used as received. The ammonia solution, 28% (14.5 M NH_4OH) was obtained from Ajax and the ammonium reagents were obtained from Sigma-Aldrich and used as received. IR spectra in the region 4000-650 cm^{-1} were recorded for finely ground powdered samples using an Agilent Cary 630 ATR instrument with ResPro data handling software. Medium or greater intensity absorptions are listed for the region 1700-650 cm^{-1}; full spectra are given in the Supporting Information Room temperature PXRD on finely ground samples were obtained on a Bruker D8Advance Eco instrument using Cu radiation (λ = 1.5406 Å) and are included in the Supporting Information. Simulated patterns from the crystal structure data were calculated using Mercury v4.3.0. Elemental analyses were performed in duplicate by the Campbell Microanalytical Laboratories, University of Otago, NZ or by the Monash Analytical Platform, Monash University, Australia.

Single Crystal X-ray Diffraction X-ray diffraction data were collected at 123 K on a Rigaku Synergy S diffractometer using either CuKα (λ = 1.54184 Å) or MoKα (λ = 0.71073 Å) radiation. Data were processed, including an absorption correction, using the proprietary software package CrysAlisPro[46] and the structures were solved and refined by conventional methods using the SHELX software suite.[47] Non-hydrogen atoms were refined with anisotropic displacement parameters and hydrogen atoms attached to carbon were placed in calculated positions. The positions of all acidic hydrogen atoms were located in the difference Fourier maps and freely refined or refined with restrained X-H distances. For compound **4**, one of the $PO_2(OH)$ groups was modelled with the hydrogen atom at half occupancy, forming a disordered P-OH···O-P system with its symmetry equivalent. For charge balance, the other component of the disorder was modelled as a half occupied H_3O^+, disordered over a crystallographic symmetry site, resulting in the following structural model: $[NH_4]_4[OH_3][LH_3][LH_2]\cdot 8(H_2O)$. The structure of alendronic acid, $LH_5\cdot H_2O$ has been determined previously at RT;[15] we have re-determined the structure at 123 K for direct comparison with the current data. Crystal data and refinement details are listed in Tables 1 and 2 and in the Supporting Information, with CCDC numbers 2100232-2100238.

Syntheses of $[NH_4][LH_4]\cdot 2(H_2O)$ 1a, 1b Aqueous ammonia (28%, *ca* 0.75 mL, 11 mmol) was added dropwise to a suspension of $LH_5\cdot H_2O$ (2.67 g, 10.0 mmol) in *ca* 20 mL of hot water and the mixture was stirred and heated for 1 h. The resulting clear and colourless solution had a pH *ca* 5. A few drops of DMF were added to the hot solution, which was then cooled to room temperature and allowed to stand overnight. The resulting colourless oil was separated from the supernatant solution and triturated with EtOH giving $[NH_4][LH_4]\cdot 2(H_2O)$ (phase 1, **1a**) as a white powder that was collected by filtration and dried in air (yield 1.73 g, 57%). FTIR (1700-650 cm^{-1}): 1625m, 1542m, 1486m, 1448m, 1414m, 1203m, 1141m, 1051vs, 1038vs, 956m, 909s, 857m, 836m,746m. $C_4H_{20}N_2O_9P_2$ (302.16); C 15.95 (calc. 15.84); H 7.02 (6.55); N 9.24 (9.21) %. The PXRD of the bulk material was consistent with that calculated from the crystal structure (see Supporting Information).

In an alternative synthesis, solid $(NH_4)_2CO_3$ (notional composition as the double salt $NH_4HCO_3{:}NH_4CO_2NH_2$, *ca* 0.40 g) was added to a suspension of $LH_5\cdot H_2O$ (2.67 g, 10.0 mmol) in *ca* 40 mL of hot water to a final pH of *ca* 5. Vigorous gas evolution was observed and a clear and colourless solution was obtained after several minutes. DMSO (*ca* 5 mL) was added in portions until a cloudy solution had formed which was heated until clear then cooled overnight. A mass of colourless crystals of impure **1a** formed which were collected by filtration and dried in air (yield 1.42 g, 47%). PXRD of the bulk product indicated that the impurity was unreacted $LH_5\cdot H_2O$. The supernatant from above deposited further crystals of $[NH_4][LH_4]\cdot 2(H_2O)$ on standing, which were shown to be a mixture of **1a** and **1b** by hand picking of the crystals (yield 0.86 g, 28%), and confirmed from the PXRD of the bulk product by comparison with the patterns calculated from the crystal structures. (see Supporting Information).

In a third synthesis, solid NH_4HCO_3 (0.80g, 10 mmol) was added to a suspension of $LH_5\cdot H_2O$ (2.67 g, 10.0 mmol) in *ca* 20 mL of hot water. Vigorous gas evolution was observed, and the resulting clear and colourless solution was stirred and heated for 1 h. The solution was then cooled to room temperature and the volume was reduced to *ca* 10 mL followed by addition of 1-2 mL of ethanol. Standing over several days yielded colourless prisms of $[NH_4][LH_4]\cdot 2(H_2O)$ (phase 1, **1a**) in two batches which were collected by filtration and dried in air (combined yield 2.19 g, 73%). FTIR (1700-650 cm^{-1}): 1625m, 1543m, 1487m, 1454m, 1415m, 1204m, 1141m, 1051vs, 1038vs, 957m, 908s, 858m, 833m, 746m, 664w. $C_4H_{20}N_2O_9P_2$ (302.16); C 15.95 (calc. 15.95); H 7.02 (6.87); N 9.24 (9.29) %. The PXRD of the bulk material was consistent with that calculated from the crystal structure (see Supporting Information).

Syntheses of $[NH_4]_2[LH_3]\cdot 3(H_2O)$ 2 Aqueous ammonia (28%, *ca* 2.0 mL, 30 mmol) was added dropwise to a heated suspension of $LH_5\cdot H_2O$ (2.67 g, 10.0 mmol) in *ca* 40 mL of water, to a final pH of 9-10. The resulting clear colourless solution was stirred and heated for 1 h, then *ca* 5 mL of EtOH was added and the mixture was allowed to cool to room temperature overnight. A large amount of colourless very fine needles formed, comprising a mixture of $[NH_4]_2[LH_3]\cdot 6(H_2O)$ (**3**) and $[NH_4]_4[OH_3][LH_3][LH_2]\cdot 8(H_2O)$ (**4**), which were collected by filtration and dried in air (yield 2.91 g, 80%). FTIR (1700-650 cm^{-1}): 1672w, 1534w, 1459m, 1439m, 1432m, 1400w, 1077vs, 1045vs, 1020m, 984m, 922m, 683w, 660w. Found: C 12.92; H 8.00; N 11.72 % (calc. for (**3**) $C_4H_{31}N_3O_{13}P_2$ (391.26); C 12.28; H 7.99; N 10.74 %; calc. for (**4**) $C_8H_{56}N_6O_{23}P_4$ (354.24); C 13.19; H 7.75; N 11.54 %). The PXRD of the isolated and dried solid confirmed the presence of both phases by comparison with the patterns calculated from the crystal structures (see Supporting Information).

The initial product mixture obtained above (1.75 g) was dissolved in *ca* 30 mL of hot water and *ca* 5 mL of DMSO was added and the mixture was cooled to room temperature overnight. Colourless plates of $[NH_4]_2[LH_3]\cdot 3(H_2O)$ (**2**) formed after several days and were collected by filtration and dried in air (yield 1.16g, 72%). IR (1700-650 cm^{-1}): 1672m, 1544m, 1432s, 1356m, 1262m, 1189w, 1074vs, 1047s, 983vs, 917m, 822w. $C_4H_{25}N_3O_{10}P_2$ (337.21); C 14.58 (calc. 14.25); H 7.50 (7.47); N 12.47 (12.46) %.

In an analogous synthesis, a larger excess of aqueous ammonia (28%, *ca* 10.0 mL, 0.15 mol) was added dropwise to a heated suspension of $LH_5\cdot H_2O$ (2.67 g, 10.0 mmol) in *ca* 40 mL of water, to a final pH of 12. The resulting clear colourless solution was stirred and heated for 1 h, then *ca* 5 mL of DMSO was added and the mixture was allowed to cool to room temperature overnight. Colourless crystals of $[NH_4]_2[LH_3]\cdot 3(H_2O)$ **2** formed and were collected by filtration, washed with EtOH (5 mL) and dried in air (yield 1.96 g, 58%). The identity of the product was established by PXRD.

Syntheses of $[NH_4]_3[LH_2]\cdot 3(H_2O)$ 5 Solid $LH_5\cdot H_2O$ (2.67 g, 10.0 mmol) was treated with aqueous ammonia (28%, 40 mL) and the mixture was stirred and heated for 20 min giving a voluminous white precipitate. The precipitate was collected by filtration and washed with aq. NH_3 (*ca* 5 mL) then dried in air for 24 h giving $[NH_4]_3[LH_2]\cdot 3(H_2O)$ (**5**) as a white powder (yield 3.27g, 92%). FTIR (1700-650 cm^{-1}): 1671w, 1523w, 1443s, 1262w, 1168w, 1078s, 1041vs, 956s, 924m, 802w, 723w, 660w. $C_4H_{28}N_4O_{10}P_2$ (354.24); C 13.56 (calc. 13.56); H 8.03 (7.98); N 14.66 (15.82) %. The solid was stored in a sealed vial and periodically examined by PXRD; after 1 month, there was significant conversion to **4** (see below).

Crystals of $[NH_4]_3[LH_2]\cdot 3(H_2O)$ (**5**) were obtained from an analogous preparation where the initial precipitate and supernatant solution were allowed to stand for two days during which the precipitate had transformed into colourless crystals. Visual examination indicated the presence of at least two crystal forms: (a) larger block-shaped prisms of **5** and (b) rectangular needles which were hand-picked and identified as $[NH_4]_4[OH_3][LH_3][LH_2]\cdot 8(H_2O)$ (**4**). The remainder of the crystals were collected by filtration and dried in air (yield 1.76g). PXRD of this material confirmed the presence of both phases. A second preparation was allowed to stand for five days prior to filtration which gave a lower yield (0.43g) of the solid mixture of compounds. A sample of these crystals was removed prior to filtration and a further crystal form was observed as small flat prisms which were identified as $[NH_4]_2[LH_3]\cdot 6(H_2O)$ (**3**), in addition to crystals of **4** and **5**. The PXRD of the isolated and dried solid confirmed the presence of all three phases. Evaporation of the filtrate after separation of the solid yielded **2** as colourless crystals (yield 1.89 g, 56%).

Acknowledgements

N.B.G. gratefully acknowledges financial support through the Faculty of Science, Monash University for a Deans Scholarship. We also acknowledge the use of the powder X-ray facilities administered by the Monash X-ray Platform.

Keywords: pharmaceuticals • bisphosphonates • structures • hydrogen-bonding

Table 1. Crystal and refinement data for **1a**, **1b** and **2**.

	1a	**1b**	**2**
Formula	$C_4H_{20}N_2O_9P_2$	$C_4H_{20}N_2O_9P_2$	$C_4H_{25}N_3O_{10}P_2$
M	302.16	302.16	337.21
Crystal System	Monoclinic	Monoclinic	Monoclinic
Space Group	$P2_1/c$	$C2/c$	$P2_1/c$
a, Å	6.7094(1)	28.7079(3)	15.1804(2)
b	12.5793(2)	6.9656(1)	8.6250(1)
c	14.2592(1)	24.7187(2)	11.5390(2)
α, °	90	90	90
β	97.401(1)	91.540(1)	110.171(2)
γ	90	90	90
V, Å^3	1193.44(3)	4941.16(10)	1418.15(4)
Z	4	16	4
d_{calcd}, g.cm^{-3}	1.682	1.625	1.579
μ, mm^{-1}	3.759	3.631	3.299
N_{total}	12352	16389	12803
N (R_{int})	2486 (0.041)	4963 (0.024)	2924 (0.042)
N_{obs} ($I > 2\sigma I$)	2355	4703	2676
$R1$ ($F^2 > 2\sigma F^2$)	0.0296	0.0273	0.0305
$wR2$ (F^2)	0.0792	0.0739	0.0826
S	1.063	1.044	1.066
parameters	210	419	248
restraints	0	0	0
$\Delta\rho$, e.Å^{-3}	0.46, -0.38	0.37, -0.39	0.41, -0.40

Table 2. Crystal and refinement data for **3**, **4** and **5**.

	3	**4**	**5**
Formula	$C_4H_{31}N_3O_{13}P_2$	$C_8H_{56}N_6O_{23}P_4$	$C_4H_{28}N_4O_{10}P_2$
M	391.26	728.46	354.24
Crystal System	Triclinic	Triclinic	Monoclinic
Space Group	P-1	P-1	$P2_1/c$
a, Å	6.7208(2)	6.6930(2)	14.6255(1)
b	10.6141(3)	9.3463(2)	8.7536(1)
c	12.2991(4)	13.1020(3)	11.6363(1)
α, °	105.464(3)	104.812(2)	90
β	92.361(3)	94.985(2)	102.961(1)
γ	95.653(2)	92.165(2)	90
V, Å^3	839.40(5)	787.83 (3)	1451.79(2)
Z	2	1	4
d_{calcd}, g.cm^{-3}	1.548	1.535	1.621
μ, mm^{-1}	3.005	0.334	3.270
N_{total}	9300	12059	15276
N (R_{int})	3392 (0.039)	4481 (0.027)	3009 (0.044)
N_{obs} ($I > 2\sigma I$)	3115	3834	2826
$R1$ ($F^2 > 2\sigma F^2$)	0.0356	0.0307	0.0285
$wR2$ (F^2)	0.1008	0.0815	0.0774
S	1.061	1.033	1.049
parameters	299	286	269
restraints	0	4	0
$\Delta\rho$, e.Å^{-3}	0.58, -0.50	0.42, -0.39	0.52, -0.46

[1] *Handbook of Pharmaceutical Salts; Properties, Selection and Use* (Eds. P. H. Stahl and C. G. Wermuth), Wiley-VCH, Weinheim, **2002**.
[2] B. Bhattacharya, A. Mondal, S. R. Soni, S. Das, S. Bhunia, K. B. Raju, A. Ghosh, C. M. Reddy, *CrystEngComm* **2018**, *20*, 6420-6429.
[3] J. L. Shamshina, S. P. Kelly, G. Gurau, R. D. Rogers, *Nature* **2015**, 528, 188-189.
[4] K. S. Egorova, E. G. Gordeev, V. P. Anaikov, *Chem. Rev*. **2017**, *117*, 7132-7189.
[5] R. G. G. Russell, *Ann. N. Y. Acad. Sci.* **2006**, *1068*, 367-401.
[6] J.-M. Rondau, F. Bitsch, E. Bourgier, M. Geiser, R. Hemming, M. Kroemer, S. Lehmann, P. Ramage, S. Rieffel, A. Strauss, J. R. Green, W. Jahnke, *ChemMedChem* **2006**, *1*, 267-273.
[7] K. L. Kavanagh, K. Guo, J. E. Dunford, X. Wu, S. Knapp, F. H. Ebetino, M. J. Rogers, R. G. G. Russell, U. Oppermann, *Proc. Natl. Acad. Sci.* **2006**, *103*, 7829-7834.
[8] R. Coleman, *Ann. N. Y. Acad. Sci.* **2011**, *1218*, 3-14.
[9] E. Oldfield, *Acc. Chem. Res*. **2010**, *43*, 1216-1226.
[10] B. Demoro, F. Caruso, M. Rossi, D. Benítez, M. González, H. Cerecetto, M. Galizzi, L. Malayil, R. Docampo, R. Faccio, A. W. Mombrú, D. Gambino, L. Otero, *Dalton Trans.* **2012**, *41*, 6468-6476.
[11] A. Saad, W. Zhu, G. Rosseau, P. Mialane, J. Marrol, M. Haouas, F. Taulelle, R. Dessapt, H. Serier-Brault, E. Rivíere, T. Kubo, E. Oldfield, A. Dolbecq, *Chem. Eur. J*. **2015**, 10537-10547.
[12] M. Cipriani, S. Rostál. León, Z- H. Li, J. S. Gancheff, U. Kemmerling, C. O. Azar, S. Etcheverry, R. Docampo, D. Gambino, L. Otero, *J. Bio. Inorg. Chem.* **2020**, *25*, 509-519.
[13] A. Ezra and G. Golomb, *Adv. Drug. Delivery Res*. **2000**, *42*, 175-195.
[14] G. Hägele, Z. Szakács, J. Ollig, S. Hermens, C. Pfaff, *Heteroatom Chem.* **2000**, *11*, 562-582.

[15] Y. Leroux, D. El Manouni, A. Safsaf, A. Neuman, H. Giller, *Phosphorus, Sulfur and Silicon Relat. Elem.* **1991**, *63*, 181-191.
[16] J. Ohanessian, D. Avenel, D. El Manouni, M. Benramdane, *Phosphorus, Sulfur and Silicon Relat. Elem.* **1997**, *129*, 99-110.
[17] L. M. Shkol'nikova, S. S. Stotman, E. G. Afonin, *Krystallografiya* **1990**, *35*, 1442.
[18] D. Vega, R. Baggio, M. T. Garland, *Acta Crystallogr., Sect. C* **1996**, *52*, 2198-2201.
[19] D. Fernandez, D. Vega, A. Goeta, *Acta Cryst., Sect. C* **2003**, *59*, m543.
[20] M. Asnani, K. Vyas, A. Bhattacharya, S. Devarakonda, S. Chakraborty, A. K. Mukherjee, *J. Pharm. Sci.* **2009**, *98*, 2113-2121.
[21] G. B. Deacon, N. B. Greenhill, P. C. Junk, M. Weiko, *J. Coord. Chem.* **2011**, *64*, 179-185.
[22] G. B. Deacon, C. M. Forsyth, N. B. Greenhill, P. C. Junk, J. Wang, *Cryst. Growth Des.* **2015**, *15*, 4646-4662.
[23] D. Vega, D. Fernández, J. A. Ellena, , *Acta Crystallogr., Sect. C* **2002**, *58*, m77-m80.
[24] K. Stahl, S. P. Treppendhal, H. Preikschat, E. Fischer, *Acta Crystallogr., Sect. E* **2005**, *61*, m132-m134.
[25] D. Liu, S. A. Kramer, R. C. Huxford-Phillips, S. Wang, J. Della Rocca, W. Lin, *Chem. Commun*. **2012**, *48*, 2668-2670.
[26] E. Boanini, P. T. M. Gazzano, M. Fini, A. Bigi, *Adv. Mater.* **2013**, *25*, 4605-4611.
[27] E. Alvarez, A. G. Marquez, T. Devic, N. Steunou, C. Serre, C. Bonhomme, C. Gervias, I. Izquierdo-Barba, M. Vallet-Regi, D. Laurencin, M. Mauri, P. Horcajada, *CrystEngComm* **2013**, *15*, 9899-9905.
[28] M. Vasaki, K. E. Papathanasiou, C. Hadjicharalambous, D. Chandrinou, P. Turhanen, D. Choquesillo-Lazarte, K. Demadis, *Chem. Commun.* **2020**, *56*, 5166-5169.
[29] G. Q. Vélez, L. Carmona-Sarabia, W. A. Rodriguez-Silva, A. A. R. Raices, L. F. Cruz, T. Hu, E. Peterson, V. López-Mejías, *J. Mater. Chem. B* **2020**, *8*, 2155-2168.
[30] B. Sridhar, K. Ravikumar, *Acta Crystallogr., Sect. C* **2011**, *67*, o115-o119.
[31] B. Sridhar, K. Ravikumar, B. Varghese, *Acta Crystallogr., Sect. C* **2014**, *70*, 67-74.
[32] G. B. Deacon, C. M. Forsyth, N. B. Greenhill, P. C. Junk, *CrystEngComm* **2017**, *19,* 5611-5621.
[33] S. Teixeira, M. M. Santos, R. Ferraz, C. Prudêncio, M. H. Fernandes, J. Costa-Rodrigues, L. C. Branco, *ChemMedChem* **2019**, *14*, 1767-1770.
[35] S. Teixeira, M. M. Santos, M. H. Fernandes, J. Costa-Rodrigues, L. C. Branco, *Pharmaceutics* **2020**, *12*, 293-303.
[35] P. Gilli, L. Pretto, V. Bertolasi, G. Gilli, *Acc. Chem. Res.* **2009**, *42*, 33-44.
[36] F. H. Allen, P. R. Raithby, G. P. Shields, R. Taylor, *Chem. Commun.* **1998**, 1043-1044.
[37] M. C. Etter, J. C. MacDonald, J. Bernstein, *Acta Crystallogr. Sect. B* **1990**, *46*, 256-262.
[38] A survey of the Cambridge Structural Database (v 2020.3, inclusive of the Feb 2021 update),[35] for systems containing the bisphosphonate moiety (excluding structures containing metals) with at least one intermolecular P-OH donor and a -PO_3 acceptor (158 entries) indicated approximately 50% had the cyclic $\boldsymbol{R}_2^2(8)$ motif and 50% had the $\boldsymbol{R}_2^2(12)$ motif, and approximately 25% had both.
[39] C. R. Groom, I. J. Bruno, M. P. Lightfoot, S. C. Ward, *Acta Crystallogr. Sect. B* **2016**, *72*, 172-179.
[40] H. Shmeeda, Y. Amitay, J. Gorin, D. Tzemach, L. Mak, S. T. Stern, Y. Barenholz, A. Gabizon, *J. Drug Target.* **2016**, *24*, 878-889.
[41] S. Edmonds, A. Volpe, H. Shmeeda, A. C. Parente-Pereira, R. Radia, J. Banuña-Torres, I. Szanda, G. W. Severin, L. Livieratos, P. J. Blower, J. Maher, G. O. Fruhwirth, A. Gabizon, R. T. M. de Rosales, *ACS Nano*, **2016**, *10*, 10294-10307.
[42] K. Stahl, J. Oddershede, H. Preikschat, E. Fisher and J. S. Bennekou, *Acta Crystallogr., Sect. C* **2006**, *62*, m112-m115.
[43] M. Silorska and J. Chojnacki, *J. Cryst.*, 2013, 741483.
[44] T. Steiner, *Angew. Chem. Int. Ed.* **2002**, *41*, 48-76.
[45] A. Sarker, I. Cukrowski, *Acta Crystallogr., Sect. E* **2011**, *67*, o2980.
[46] *CrysAlisPro v 1.171.40.49a*, Rigaku Oxford Diffraction, Yarnton, England, **2019**.
[47] G. M. Sheldrick, *SHELX-2014*, *Acta Crystallogr., Sect. C: Struc. Chem.* **2015**, *71*, 3-8.

ARTICLE

Entry for the Table of Contents (Please choose one layout)

Layout 1:

FULL PAPER

Six crystal structures of ammonium salts of 4-aminium-1-hydroxybutylidine)-1,1-bisphosphonic acid (alendronic acid) show complex 3-D supramolecular networks derived from the large number of competing O-H···O and N-H···O synthons. However, substructure motifs such as such as 2-D sheets, zig-zag chains and ladder-like arrays were observed correlating with the ionisation level of the parent acid.

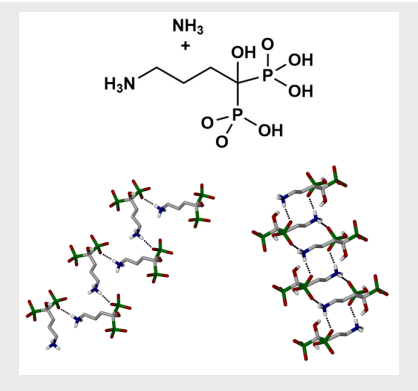

*Author(s), Corresponding Author(s)**

Page No. – Page No.

Title

Layout 2:

FULL PAPER

*Author(s), Corresponding Author(s)**

Page No. – Page No.

Title

Text for Table of Contents

Additional Author information for the electronic version of the article.

Author: ORCID identifier
Author: ORCID identifier
Author: ORCID identifier